Tetrahedron 69 (2013) 9675–9681

Contents lists available at ScienceDirect

Tetrahedron

journal homepage: www.elsevier.com/locate/tet

Experimental and computational study of intermolecular migration of *N*,*N*-dimethylcarbamoyl group from N(7) to N(1) on a 7-azaindoline derivative

Yoshiharu Uruno [a], Akio Tanaka [b], Kazuki Hashimoto [c], Shinya Usui [a], Yasunao Inoue [a,d], Yasuko Konishi [a], Atsushi Suwa [a], Kentaro Takai [a], Wataru Katoda [c], Norio Fujiwara [a], Takaaki Sumiyoshi [a,*]

[a] *Drug Research Division, Dainippon Sumitomo Pharma Co. Ltd., 33-94 Enoki-cho, Suita, Osaka 564-0053, Japan*
[b] *Organic Synthesis Research Laboratory, Sumitomo Chemical Co. Ltd., 1-98, Kasugade-naka 3-chome, Konohana-ku, Osaka 554-8558, Japan*
[c] *Process Chemistry Research & Development Laboratories, Dainippon Sumitomo Pharma Co. Ltd., 1-98, Kasugade-naka 3-chome, Konohana-ku, Osaka 554-8558, Japan*
[d] *R & D Department, DSP Gokyo Food & Chemical Co. Ltd., 33-94 Enoki-cho, Suita, Osaka 564-0053, Japan*

ARTICLE INFO

Article history:
Received 19 June 2013
Received in revised form 6 September 2013
Accepted 7 September 2013
Available online 14 September 2013

Keywords:
7-Azaindoline
N,*N*-Dimethylcarbamoylation
Intermolecular migration
Muscarinic acetylcholine receptors agonist
DFT calculation

ABSTRACT

N,*N*-Dimethylcarbamoylation of the anilinic nitrogen atom N(1) on the spiro 7-azaindoline consists of two steps. The first step is *N*,*N*-dimethylcarbamoylation of the pyridyl nitrogen atom N(7), leading to the formation of an isolable intermediate. The second step is intermolecular migration of the *N*,*N*-dimethylcarbamoyl group from the pyridyl nitrogen atom N(7) to the anilinic nitrogen atom N(1). We accomplished optimization of the reaction conditions based on the revealed reaction mechanism and a large scale synthesis of compound **3** in quantitative yield.

1. Introduction

Indoline is one of the common scaffolds used in medicinal chemistry.[1] In particular, spiroindoline is frequently used to identify ligands for G-protein-coupled receptors as well as various enzymes.[2] Pfizer medicinal chemists have recently reported that transformation of indolines to azaindolines can minimize the risk of adverse drug reactions (ADRs) associated with the use of indolines.[3] This report suggests that replacement of indolines by azaindolines reduces electron density and reactivity of the benzene ring and suppresses *N*-nitrosation and oxidation of reactive metabolites (Fig. 1).

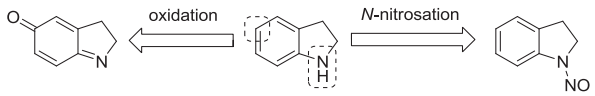

Fig. 1. Plausible metabolic pathways for indolines ADRs.

These findings support the idea that azaindoline derivatives are useful scaffolds for identification of ligands with high pharmacological activity and low ADRs. On the other hand, replacement of indolines by azaindolines is also reported to lower reactivity of the anilinic nitrogen atoms.[4] In addition, there are only few reports describing metabolic modification of azaindolines anilinic nitrogens.[5] Even with these drawbacks, it is still important to develop new synthetic methods for the preparation of azaindolines as scaffolds for safer drug candidates.

In our drug discovery program, we have found the 7-azaindoline derivative **1** as a muscarinic acetylcholine receptors (mAChRs) agonist selective for M_1 and M_4 mAChRs over M_2, M_3 and M_5 (Fig. 2). Clinical trials with xanomeline demonstrated that M_1 and M_4 mAChRs are attractive therapeutic targets for Alzheimer's disease and schizophrenia.[6]

In our synthesis of compound **1**, we found that formation of urea at the anilinic nitrogen atom of 7-azaindoline provided a low yield. To overcome this problem, we focused on clarifying the mechanism of carbamoylation by isolation of the reaction intermediate and calculation of density functional theory (DFT). Here we describe a rational optimization of the reaction conditions for practical

* Corresponding author. Tel.: +81 6 6337 5906; e-mail address: takaaki-sumiyoshi@ds-pharma.co.jp (T. Sumiyoshi).

0040-4020/$ – see front matter © 2013 Elsevier Ltd. All rights reserved.
http://dx.doi.org/10.1016/j.tet.2013.09.024

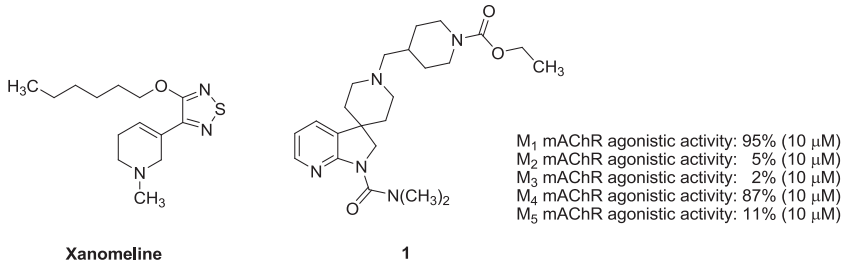

Fig. 2. Structures of xanomeline and compound **1**.

synthesis of compound **1**. Our efforts revealed that intermolecular migration of the *N*,*N*-dimethylcarbamoyl group from the pyridyl nitrogen atom to the anilinic nitrogen atom is a rate-determining step. Based on this finding, we optimized reaction concentrations and temperature effectively and used the optimized procedure to large scale synthesis of compound **1**.

2. Results and discussion

The initial synthetic route of compound **1** is shown in Scheme 1. Reaction of the known 7-azaindoline compound **2** (1.0 equiv) with *N*,*N*-dimethylcarbamoyl chloride (1.2 equiv) in the presence of triethylamine (3.0 equiv) in toluene (0.2 M) at 90 °C for 24 h afforded compound **3** in only 28% isolated yield. When excess amounts of reagents were used, i.e., *N*,*N*-dimethylcarbamoyl chloride (4.0 equiv) and triethylamine (8.0 equiv) in toluene (0.2 M) at 90 °C for 24 h, the yield of compound **3** increased to 68%. However, reproducibility of this yield was poor.

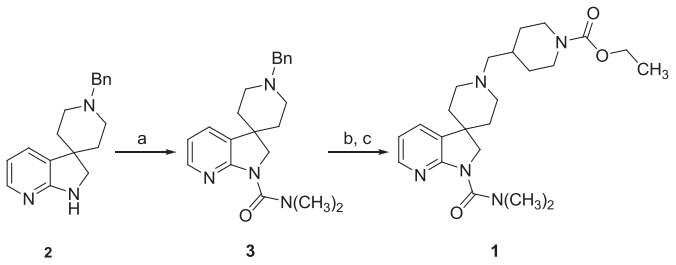

Scheme 1. Synthesis of the selective M_1 and M_4 mAChRs agonist **1**.Reagents and conditions: (a) *N*,*N*-Dimethylcarbamoyl chloride (1.2 equiv), triethylamine (3.0 equiv), toluene (0.2 M), 90 °C (28%); (b) $HCOONH_4$, 10% Pd/C, CH_3OH, reflux (99%); (c) Ethyl 4-formylpiperidine-1-carboxylate, $NaBH(OCOCH_3)_3$, CH_3COOH, CH_2Cl_2, rt (75%).

Thin layer chromatography (TLC) analysis (Fig. 3A) revealed that the reaction consisted of two steps. In the first step, the spot of the starting material **2** (R_f=0.4) was quickly converted to a polar spot (R_f=0.2). In the second step, the polar spot decreased gradually, giving rise to the spot of the target compound **3** (R_f=0.6). The polar unknown compound was also observed in HPLC analysis (Fig. 3B). LCMS analysis indicated that both compound **3** and the intermediate had the same molecular weight (m/z=351). In order to determine the structure of the intermediate, we tried to isolate it. Fortunately, base-free conditions enabled isolation of 2HCl salt of intermediate compound **4** in 51% yield (Scheme 2).

^{1}H NMR spectrum of the intermediate **4** shows no aromatic ring structure. Chemical shifts of the protons at the pyridine ring of compound **2** shifted from 7.8, 7.3 and 6.5 ppm to 6.7, 6.3 and 5.6 ppm, respectively, in the spectrum of compound **4** (Fig. 4A and B). These lower chemical shifts shifted back to 8.1, 7.4 and 6.8 ppm

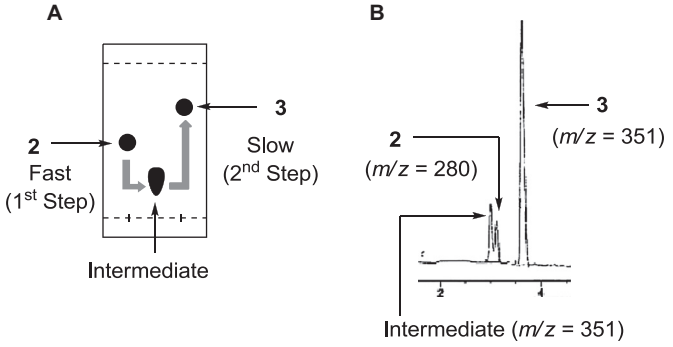

Fig. 3. TLC analysis (A) and HPLC analysis (B) of *N*,*N*-dimethylcarbamoylation. TLC analysis conditions (Silicagel: FUJI SILYSIA, TLC Plates NH, eluent: ethyl acetate); HPLC conditions (Column: Eclipse Plus C_{18} 4.6×100 mm, 3.5 μm; flow 1.0 mL/min; Eluent: Gradient 10–90% methanol in water containing 0.01% TFA).

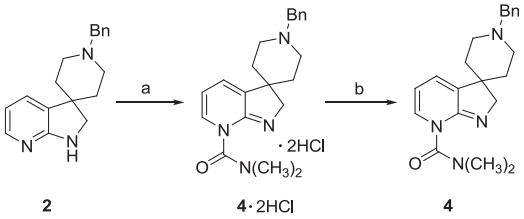

Scheme 2. Isolation of the Key Intermediate **4**. Reagents and conditions: (a) *N*,*N*-Dimethylcarbamoyl chloride (1.5 equiv), toluene, 90 °C (51%); (b) Na_2CO_3, H_2O, rt (99%).

in the ^{1}H NMR spectrum of compound **3** (Fig. 4C). These results strongly indicate that intermediate **4** was produced through *N*,*N*-carbamoylation of the pyridyl nitrogen atom on 7-azaindoline. As migration of the *N*,*N*-dimethylcarbamoyl group must have happened to allow production of compound **3** from compound **2** through compound **4**, we investigated whether this migration was intramolecular or intermolecular by DFT calculation (Fig. 5).[7]

DFT calculation was carried out using the Gaussian09 package.[8] The hybrid functional B3LYP[9] combined with 6-31+G(d,p)[10] basis set specifying 6d functions was used to fully optimize the geometry of stable molecules and transition state structures. All transition states were confirmed by IRC calculation. In order to reduce calculation cost, 3-spiro-linked piperidyl-7-azaindoline (**SM1**) was used as a model substrate (Fig. 6). Through careful exploration of rearrangement pathways from compound **SM1** to **TM1**, four mechanistic pathways were identified (Fig. 6). The structures of the transition states and intermediates are also shown in Supplementary data (Fig. S1).

In the intramolecular pathway, mechanistic route 1 shows **SM1** carbamoyl group migration via **TS1** to form **TM1** (Fig. 6). The Gibbs activation energy was calculated as 41.21 kcal/mol, which indicates an energetically difficult rearrangement (Fig. 7).

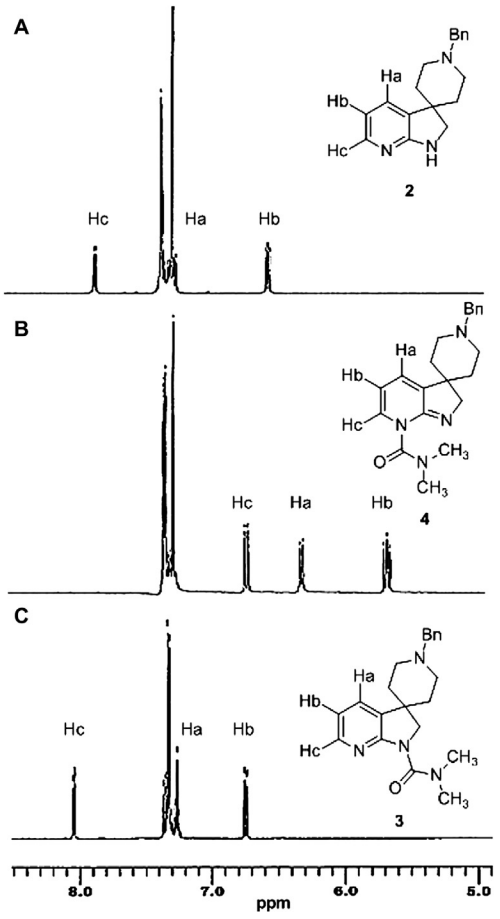

Fig. 4. ^{1}H NMR Spectra of compounds **2** (A), **4** (B) and **3** (C).

in the caged eight-membered ring. The steric hindrance and distortion cancel the thermodynamic advantage of intermolecular concerted mechanism. The route 4 is a stepwise carbamoyl group exchange between a pair of **SM1** (Fig. 6). The pathway consists of three transition states (**TS5**, **TS6** and **TS7**) and two intermediates (**IM2** and **IM3**). Initially, the pyridyl *N*-carbamoyl group in **SM1** is nucleophilically attacked by an unsubstituted anilinic nitrogen in another **SM1** via **TS5** to form the zwitterionic intermediate **IM2**. Following that, the anionic oxygen in **IM2** attacks the intramolecular urea carbon via **TS6** with six-membered ring structure to form the carbamate **IM3**, which is finally transformed into a pair of **TM1** via **TS7** with six-membered ring structure. Reaction barriers of the three transition states **TS5**, **TS6** and **TS7** with reference to **SM1** were much lower than those of the other three routes 1, 2 and 3 (24.58, 27.73 and 23.73 kcal/mol, Fig. 8). In other words, route 4 was the most plausible mechanism in the investigated pathways. The important transition states **TS6** and **TS7** were *N*-carbonyl migration from the pyridyl nitrogen atom to the anilinic nitrogen atom with a six-membered ring conformation. In the two intermolecular mechanisms, the reaction barrier of the concerted route 3 was higher because of repulsion between the two caged tetrahedral carbons in **TS4**. In contrast, route 4 avoids steric distortion by stepwise *N*-carbamoyl exchange via **TS6** and **TS7** to reduce reaction barrier. To confirm the proposed mechanism, we performed additional calculations to estimate the reaction barriers for **TS1**, **TS4** and **TS5** using M06-2X/6-31+G(d,p)[11] ,that is, the method to treat dispersion interactions (Fig. S2 and Table S1). The results showed the barrier of the stepwise intermolecular migration (**TS5**) was over 10 kcal/mol lower than of the intramolecular (**TS1**) and the concerted intermolecular mechanism (**TS4**), which indicated the similar fashion of the result of B3LYP method.

Since DFT calculation suggested that the reaction proceeded by an intermolecular process, we initially tried to optimize the reaction concentrations. First, a suitable concentration for the synthesis of compound **3** from compound **4** was explored in toluene at 90 °C (Table 1). Under high dilution conditions (0.002 M), the migration reaction did not proceed (Table 1, entry 1). As concentrations of the reaction increased (0.1 M to neat), the conversion ratio of compound **4** to compound **3** increased (Table 1, entries 2–6). Treatment of **4** under neat conditions afforded a conversion ratio of compound **3**:compound **2**=90:10. Under neat condition, the conversion of compound **4** to compound **3** was also observed at room temperature (entry 7). These results and LCMS monitoring study (Scheme S1) indicate that *N*,*N*-dimethylcarbamoyl group of intermediate **4** is migrated via intermolecular mechanism.

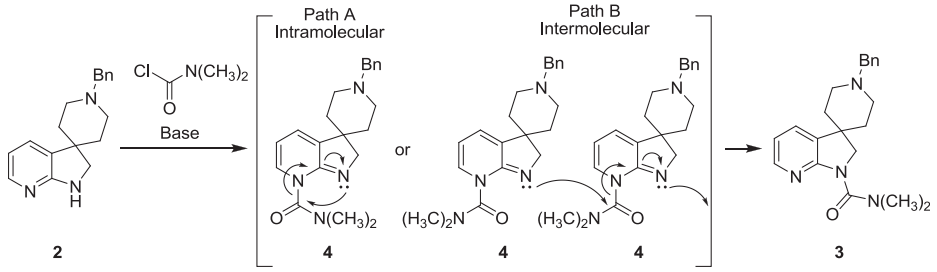

Fig. 5. Migration of the *N*,*N*-dimethylcarbamoyl group via intramolecular (path A) or intermolecular (path B) reaction.

The *N*,*N*-dimethylcarbamoyl group of **TS1** had four-membered cyclic structure to raise the reaction barrier (Fig. S1). Route 2 shows a stepwise *N*-carbamoylation of **SM1** with additional *N*,*N*-dimethylcarbamoyl chloride via **TS2** to form intermediate **IM1**, followed by elimination of *N*,*N*-dimethylcarbamoyl chloride via **TS3** to provide **TM1** (Fig. 6). The Gibbs activation energy values of **SM1** to **TS2** and **IM1** to **TS3** were 38.30 and 25.85 kcal/mol, respectively (Fig. 7).

In the two intermolecular migration mechanisms, route 3 is a concerted pathway of carbamoyl group exchange between a pair of **SM1** via **TS4** to form a pair of **TM1** (Fig. 6). The Gibbs free activation energy for this pathway was estimated to be 38.53 kcal/mol, which is almost the same as the energy for the intramolecular mechanisms (Fig. 7). **TS4** is composed of an asymmetric eight-membered ring structure with formation of two bonds (1.61 and 2.14 Å) as indicated by dash lines in Fig. S1. The asymmetry stems from steric distortion between the two nearby tetrahedral carbons

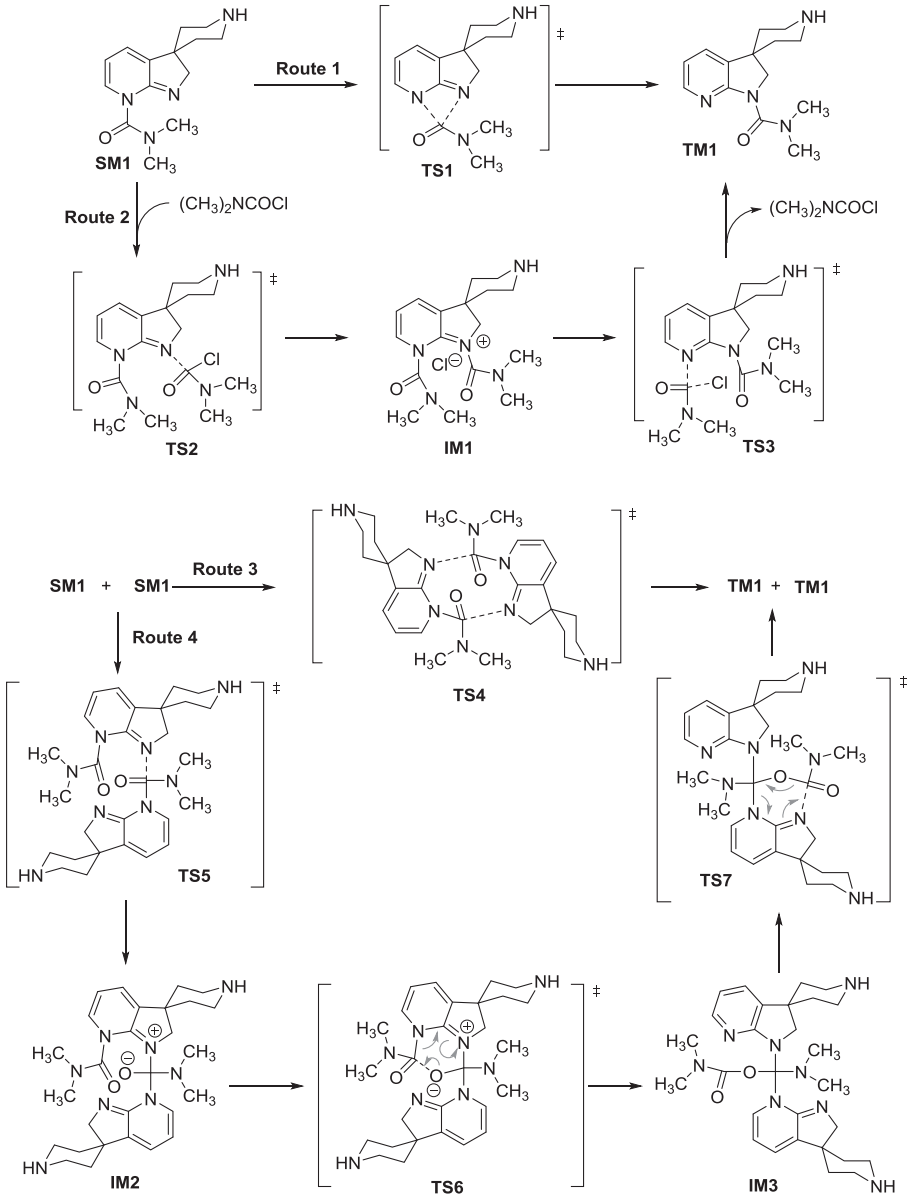

Fig. 6. Four possible pathways explored by computational study.

(Table 2, entry 1) and compound **4** was transformed to compound **3** via intermolecular migration of *N*,*N*-dimethylcarbamoyl group (Table 2, entries 2–4).

Finally, based on the results described above, we optimized the reaction conditions as shown in Table 3. We determined the optimal reaction concentration to be 2.0 M; at higher concentration agitation/mixing is insufficient for application at large scale. Reaction temperature and base were changed, from 90 °C to reflux condition, and from triethylamine to *N*,*N*-diisopropylethylamine (DIPEA) since triethylamine boiling point was only 88.8 °C as compared to 127 °C for DIPEA. As expected, the modified reaction conditions afforded the desired compound **3** in 99% yield (<1 g scale) (Table 3, entry 1). However, in case of large scale synthesis (>20 g), the isolated yield of compound **3** decreased to 84%, and the starting material **2** was recovered (Table 3, entry 2). Because of low thermal efficiency in large scale synthesis, compound **4** might decompose to the starting material **2**. To complete the reaction, 0.3 equiv of *N*,*N*-dimethylcarbamoyl chloride and 0.6 equiv of DIPEA were added to the reaction mixture after 3 h to obtain compound **3** in quantitative yield (Table 3, entry 3).

3. Conclusion

In summary, we have successfully improved the yield of the original synthesis of compound **3** through identification of the reaction mechanism, which involves intermolecular migration of *N*,*N*-dimethylcarbamoyl group as indicated by isolation of intermediate **4** and DFT calculation. Taking advantage of this method, we accomplished a large scale synthesis of the promising antipsychotic compound **1**.

4. Experimental section

4.1. General information

All reagents and solvents were purchased from commercial suppliers and used without further purification. Nuclear Magnetic Resonance (NMR) spectra were recorded at ambient temperature, operating at 400 MHz for ^{1}H NMR and 100 MHz for ^{13}C NMR. Chemical shifts were expressed in parts per million and referenced to tetramethylsilane (TMS) in $CDCl_3$ and residual solvent peak in

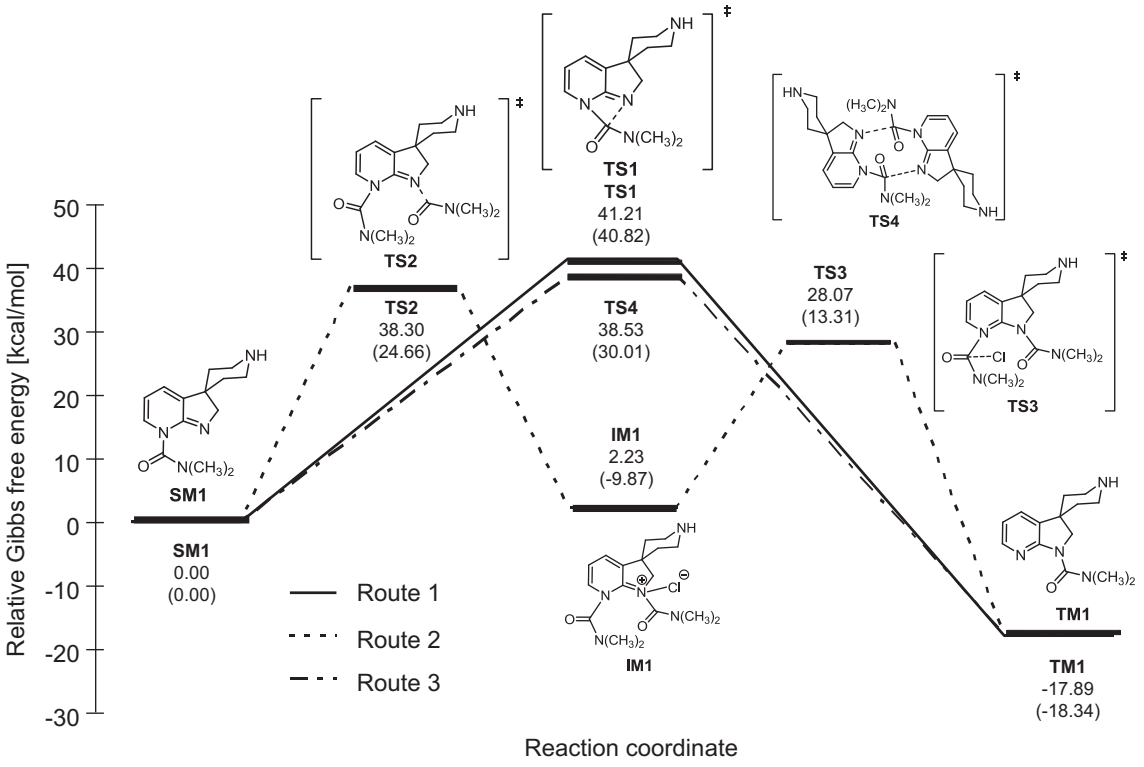

Fig. 7. Reaction coordinates for rearrangement of **SM1** to **TM1** in the mechanistic routes 1, 2 and 3. Upper numbers indicate relative Gibbs free energy, and the numbers in parentheses are relative enthalpies in units of kcal/mol.

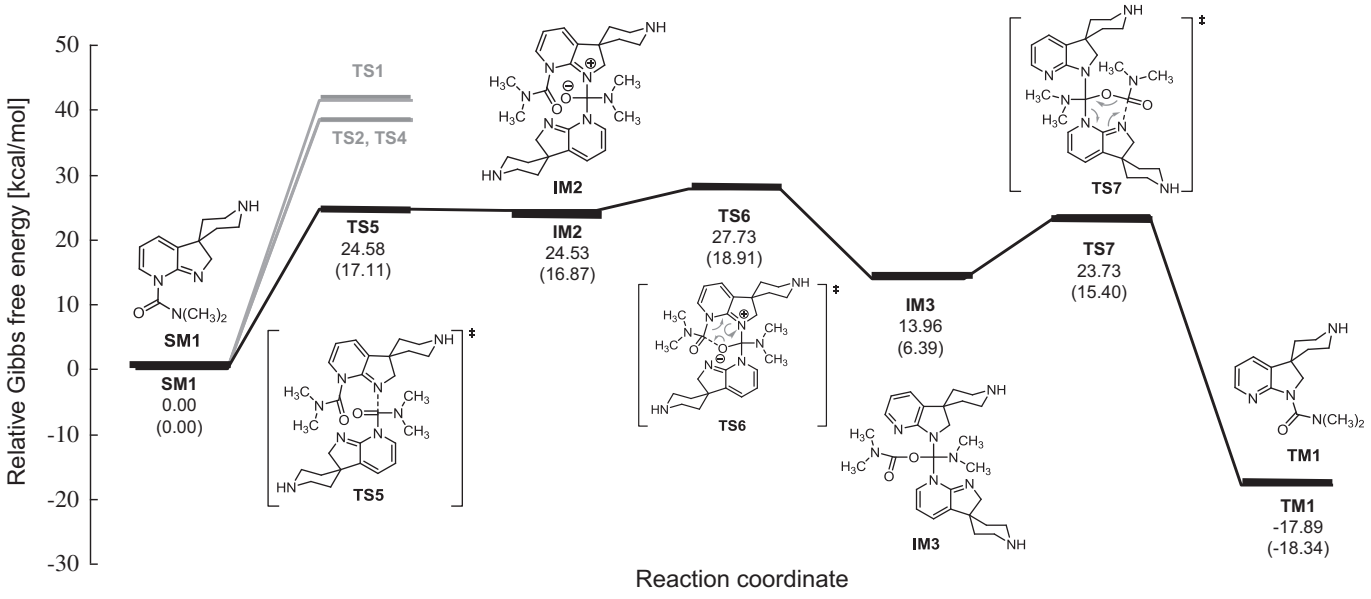

Fig. 8. Reaction coordinate of the intermolecular stepwise rearrangement mechanism (route 4) from **SM1** to **TM1**. The upper numbers indicate relative Gibbs free energy, and the numbers in parentheses are relative enthalpies in units of kcal/mol.

$CDCl_3$ or DMSO-d_6 for ^1H NMR and ^{13}C NMR. Splitting pattern designed as follows: s, singlet; d, doublet; t, triplet; q, quartet; m, multiplet; br s, broad singlet; and dd, double doublet. Mass spectra were obtained using Electro Spray Ionization. ESI mass spectra (for HRMS) were measured on a hybrid linear ion trap–Orbitrap mass spectrometer. IR spectra are reported in wavenumbers (cm^{-1}). TLC analysis was performed on TLC Plates NH. Column chromatography was carried out using prepacked amino silica gel (40 μm, 60 Å).

4.2. Synthesis

*4.2.1. 1-Benzyl-1′,2′-dihydrospiro[piperidine-4,3′-pyrrolo[2,3-b]pyridine] (**2**).* Preparation of compound **2** had been described in previous reports (Refs. 5a,b). White solid; mp 124–126 °C; ^1H NMR (400 MHz, $CDCl_3$) δ 1.72–1.75 (m, 2H), 1.85–1.94 (m, 2H), 2.10–2.15 (m, 2H), 2.82–2.85 (m, 2H), 3.45 (s, 2H), 3.55 (s, 2H), 4.42 (br s, 1H), 6.53 (dd, J=7.1, 5.1 Hz, 1H), 7.21–7.34 (m, 6H), 7.84 (dd, J=5.1, 1.5 Hz,

Table 1
Effect of reaction concentrations to migration of *N*,*N*-dimethylcarbamoyl group

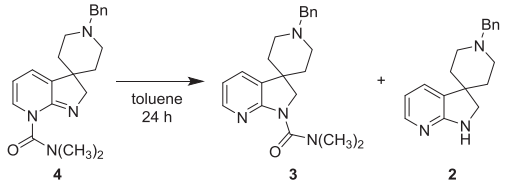

Entry	Temperature (°C)	Concentration (M)	Ratio[a]		
			4	**3**	**2**
1	90	0.002	>99	<1	<1
2	90	0.1	57	17	26
3	90	0.2	65	21	14
4	90	1	<1	56	44
5	90	2	<1	70	30
6	90	Neat	<1	90	10
7	rt	Neat	14	69	17
8	Reflux	0.2	<1	>99	<1
9	Reflux	2	<1	>99	<1

[a]Reaction ratio was determined by ^{1}H NMR.

Table 2
NMR monitoring studies

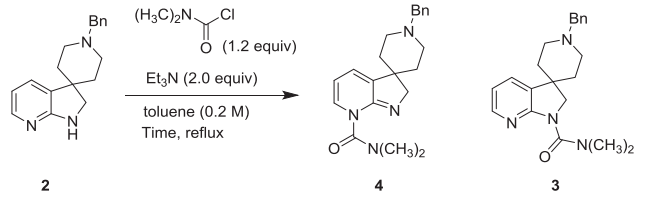

Entry	Time (h)	Ratio[a]		
		2	**4**	**3**
1	0.25	11	82	7
2	1	12	56	32
3	3	6	37	57
4	24	<1	<1	>99

[a] Reaction ratio was determined by ^{1}H NMR. The reaction was performed at a 0.7 mmol scale of compound **2**.

Table 3
Optimization of large scale synthesis of compound 3

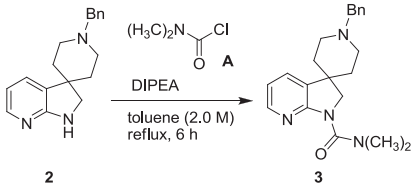

Entry	**A** (equiv)	DIPEA (equiv)	Yield (%)	Scale (g)
1	1.5	2.0	99	<1
2	1.5	2.0	84	>20
3	1.5+0.3	2.0+0.6	>99	>20

1H); ^{13}C NMR (100 MHz, $CDCl_3$) δ 36.4, 42.7, 50.2, 54.0, 63.5, 113.4, 127.1, 128.2, 129.2, 129.7, 129.9, 138.2, 146.4, 163.5; IR 694, 744, 771, 1612 cm^{-1}; MS (ESI, positive) *m*/*z* 280 $(M+H)^+$; HRMS (ESI, positive) *m*/*z* calcd for $C_{18}H_{22}N_3$ $(M+H)^+$ 280.1808, found 280.1813; Anal. Calcd for $C_{18}H_{21}N_3$: C, 77.38; H, 7.58; N, 15.04. Found: C, 77.16; H, 7.67, N, 15.06.

*4.2.2. 1-Benzyl-N,N-dimethylspiro[piperidine-4,3′-pyrrolo[2,3-b]pyridine]-1′(2′H)-carboxamide (**3**).* To a solution of *N*,*N*-diisopropylethylamine (105 mL, 752 mmol) and compound **2** (105 g, 376 mmol) in toluene (247 mL) was added *N*,*N*-dimethylcarbamoyl chloride (52 mL, 564 mmol) at room temperature and the mixture was stirred under reflux for 3 h. After addition of *N*,*N*-diisopropylethylamine (32 mL, 226 mmol) and *N*,*N*-dimethylcarbamoyl chloride (10 mL, 113 mmol), the reaction mixture was stirred for 3 h under reflux. The reaction mixture was cooled to room temperature, quenched with water and extracted with EtOAc. Organic layer was washed with saturated aqueous $NaHCO_3$ and brine, dried over Na_2SO_4 and filtered. The filtrate was concentrated in vacuo to give solid. The solid was triturated with *n*-hexane to give **3** (119 g, 99%) as a pale yellow solid. Mp 128–129 °C; ^{1}H NMR (400 MHz, $CDCl_3$) δ 1.70–1.73 (m, 2H), 1.89–1.96 (m, 2H), 2.15–2.21 (m, 2H), 2.84–2.87 (m, 2H), 3.03 (s, 6H), 3.56 (s, 2H), 3.78 (s, 2H), 6.75 (dd, *J*=7.3, 5.4 Hz, 1H), 7.26–7.35 (m, 5H), 7.36 (dd, *J*=7.3, 1.7 Hz, 1H), 8.05 (dd, *J*=5.4, 1.7 Hz, 1H); ^{13}C NMR (100 MHz, $CDCl_3$), δ 35.5, 38.1, 39.7, 50.1, 57.5, 63.3, 116.2, 127.1, 128.2, 129.2, 130.3, 132.1, 137.8, 146.4, 157.3, 157.6: IR 702, 744, 771, 1366, 1416, 1655 cm^{-1}; MS (ESI, positive) *m*/*z* 351 $(M+H)^+$; HRMS (ESI, positive) *m*/*z* calcd for $C_{21}H_{27}ON_4$ $(M+H)^+$ 351.2179, found 351.2183; Anal. Calcd for $C_{21}H_{26}N_4O$: C, 71.97; H, 7.48; N, 15.99. Found: C, 72.03; H, 7.58; N, 16.07.

*4.2.3. Ethyl 4-{[1′-(dimethylcarbamoyl)-1′,2′-dihydro-1H-spiro[piperidine-4,3′-pyrrolo[2,3-b]pyridin]-1-yl]methyl}piperidine-1-carboxylate (**1**).* To a solution of **3** (27.5 g, 78.5 mmol) in methanol (82 mL) were added $HCOONH_4$ (24.7 g, 392 mmol) and 10% palladium on carbon (5.5 g). The mixture was stirred under reflux for 7 h, cooled to room temperature and filtered. The filtrate was concentrated in vacuo. The residue was diluted with $CHCl_3$ and washed with water, saturated aqueous $NaHCO_3$ and brine. The organic layer was dried over Na_2SO_4, filtered and concentrated in vacuo to give a pale yellow amorphous (20.4 g, 99%). To a solution of the amorphous (20.4 g, 78.2 mmol) acetic acid (6.7 mL, 117 mmol) and ethyl 4-formylpiperidine-1-carboxylate (14.5 g, 78.2 mmol) in dichloromethane (390 mL) was added sodium triacetoxyborohydride (24.8 g, 117 mmol) at room temperature and the mixture was stirred for 2 h. The reaction mixture was cooled to 0 °C and quenched with saturated aqueous $NaHCO_3$. The organic layer was washed with water and brine, dried over Na_2SO_4, filtered and concentrated in vacuo. The residue was purified by silica gel column chromatography (hexane–AcOEt) to afford **1** (25.3 g, 75%) as a white solid; mp 120–122 °C; ^{1}H NMR (400 MHz, $CDCl_3$) δ 1.04–1.18 (m, 2H), 1.26 (t, *J*=7.3 Hz, 3H), 1.65–1.82 (m, 8H), 1.84–1.95 (m, 2H), 2.11 (t, *J*=10.7 Hz, 2H), 2.21 (d, *J*=7.3 Hz, 2H), 2.71–2.83 (m, 4H), 3.78 (s, 2H), 3.56 (s, 2H), 3.78 (s, 2H), 4.13 (q, *J*=7.3 Hz, 2H), 4.13–4.17 (m, 1H), 6.76 (dd, *J*=7.3, 5.4 Hz, 1H), 7.37 (dd, *J*=7.3, 1.5 Hz, 1H), 8.06 (dd, *J*=5.4, 1.5 Hz, 1H); ^{13}C NMR (100 MHz, $CDCl_3$) δ 14.7, 30.7, 33.7, 35.7, 38.2, 39.9, 43.9, 50.8, 57.5, 61.1, 64.9, 116.2, 130.4, 132.2, 146.5. 155.6, 157.3, 157.7; IR 768, 1080, 1111, 1361, 1420 cm^{-1}; MS (ESI, positive) *m*/*z* 430 $(M+H)^+$; HRMS (ESI, positive) *m*/*z* calcd for $C_{23}H_{36}O_3N_5$ $(M+H)^+$ 430.2813, found 430.2824; Anal. Calcd for $C_{23}H_{35}N_5O_3$: C, 64.31; H, 8.21; N, 16.30. Found: C, 64.15; H, 8.33, N, 16.22.

*4.2.4. 1-Benzyl-N,N-dimethylspiro[piperidine-4,3′-pyrrolo[2,3-b]pyridine]-7′(2′H)-carboxamide dihydrochloride (**4**·2HCl).* To a solution of compound **2** (200 mg, 0.72 mmol) in toluene (0.7 mL) was added *N*,*N*-dimethylcarbamoyl chloride (99 μL, 1.1 mmol) at 60 °C and the mixture was stirred for 4 h. The precipitate was collected by filtration and washed with diethyl ether to give **4**·2HCl (157 mg, 51%) as a pale yellow solid; mp 193–194 °C; ^{1}H NMR (400 MHz, DMSO-d_6) δ 2.01 (d, *J*=13.7 Hz, 2H), 2.32–2.45 (m, 2H), 2.92 (s, 3H), 3.07 (s, 3H), 3.08–3.29 (m, 4H), 3.86 (s, 2H), 4.31 (s, 2H), 6.86 (t, *J*=6.8 Hz, 1H), 7.42–7.48 (m, 4H), 7.64–7.51 (m, 2H), 7.88 (d, *J*=6.6 Hz, 1H), 10.4 (br s, 1H), 11.6 (br s, 1H); ^{13}C NMR (100 MHz, DMSO-d_6) δ 32.3, 37.2, 38.1, 40.7, 47.6, 55.5, 58.7, 112.5, 128.7, 129.3, 130.0, 131.3, 131.9, 133.8, 138.3, 149.5, 152.7; IR 768, 1080, 1111, 1203, 1362, 1420,

1667 cm^{-1}; MS (ESI, positive) *m*/*z* 351; HRMS (ESI, positive) *m*/*z* calcd for $C_{21}H_{27}ON_4$ $(M+H)^+$ 351.2179, found 351.2188; Anal. Calcd for $C_{21}H_{26}N_4O\cdot 2HCl\cdot H_2O$: C, 57.14; H, 6.85; N, 12.69; Cl, 16.06. Found: C, 56.85; H, 6.90; N, 12.54; Cl, 15.81.

*4.2.5. 1-Benzyl-N,N-dimethylspiro[piperidine-4,3′-pyrrolo[2,3-b]pyridine]-7′(2′H)-carboxamide (**4**).* An aqueous solution of **4**·2HCl (157 mg, 0.37 mmol) was basified with saturated aqueous Na_2CO_3. The mixture was stirred for 5 min and extracted with AcOEt. The organic layer was dried over Na_2SO_4, filtered, and concentrated in vacuo to give **4** (129 mg, 99%) as a pale yellow oil. ^1H NMR (400 MHz, $CDCl_3$) δ 1.56–1.82 (m, 4H), 2.02–2.15 (m, 2H), 2.76–2.86 (m, 2H), 3.05 (br s, 6H), 3.52 (s, 2H), 3.72 (s, 2H), 5.64 (t, *J*=6.2 Hz, 1H), 6.29 (d, *J*=6.2 Hz, 1H), 6.71 (dd, *J*=7.3, 1.3 Hz, 1H), 7.23–7.36 (m, 5H); ^{13}C NMR (100 MHz, $CDCl_3$) δ 35.6, 36.3, 42.8, 50.2, 63.5, 65.8, 103.9, 121.4, 127.0, 128.2, 128.9, 129.1, 138.3, 145.9, 155.0, 157.9; IR 698, 736, 1115, 1173, 1207, 1238, 1385, 1589, 1694 cm^{-1}; MS (ESI, positive) *m*/*z* 351; HRMS (ESI, positive) *m*/*z* calcd for $C_{21}H_{27}N_4O$ $(M+H)^+$ 351.2179, found 351.2187.

4.3. Computational methods

DFT calculation was carried out using the Gaussian09 package. The hybrid functional B3LYP combined with 6-31+G(d,p) basis set specifying 6d functions was used to fully optimize the geometry of stable molecules and transition state structures. Vibrational frequency analyses were used to search for transition state structures and to estimate thermochemical kinetics. Intrinsic reaction coordinate (IRC) calculation was also executed for all transition state structures to verify first-order saddle points on potential energy surface between two local minima.[12] All DFT calculations took into account a solvation model of the polarizable continuum model using the integral equation formalism variant (IEFPCM) with united atom-for-Hartree–Fock (UAHF) radii.[13] Toluene was specified as the reaction solvent for execution inputs.

Acknowledgements

We really thank Keiko Bando for elemental analyses and Naohiro Nishimura and Sayo Takayama for HRMS analyses.

Supplementary data

^1H and ^{13}C NMR spectra for compounds **1**–**4** and **4**·2HCl, Figures, Schemes, Tables and Additional materials for DFT calculations. Supplementary data related to this article can be found at http://dx.doi.org/10.1016/j.tet.2013.09.024.

References and notes

1. (a) Vu, A. T.; Cohn, S. T.; Zhang, P.; Kim, C. Y.; Mahaney, P. E.; Bray, J. A.; Grace, H.; Johnston, G. H.; Koury, E. J.; Cosmi, S. A.; Deecher, D. C.; Smith, V. A.; Harrison, J. E.; Leventhal, L.; Whiteside, G. T.; Kennedy, J. D.; Trybulski, E. J. *J. Med. Chem.* **2010**, *53*, 2051–2062; (b) Zhang, D.; Song, H.; Qin, Y. *Acc. Chem. Res.* **2011**, *44*, 447–457; (c) Marquis, K. L.; Sabb, A. L.; Sheree, F. L.; Brennan, J. A.; Piesla, M. J.; Comery, T. A.; Grauer, S. M.; Ashby, C. R., Jr.; Nguyen, H. Q.; Dawson, L. A.; Barret, J. E.; Stack, G.; Meltzer, H. Y.; Harrison, B. L.; Rosenzweig-Lipson, S. *J. Pharmacol. Exp. Ther.* **2007**, *320*, 486–496; (d) Khan, P. M.; Correa, R. G.; Divlianska, D. B.; Peddibhotla, S.; Sessions, E. H.; Magnuson, G.; Brown, B.; Suyama, E.; Yuan, H.; Mangravita-Novo, A.; Vicchiarelli, M.; Su, Y.; Vasile, S.; Smith, L. H.; Diaz, P. W.; Reed, J. C.; Roth, G. P. *ACS Med. Chem. Lett.* **2011**, *2*, 780–785; (e) Boal, B. W.; Schammel, A. W.; Garg, N. K. *Org. Lett.* **2009**, *11*, 3458–3461.
2. (a) Pong, S.-S.; Chaung, L.-Y. P.; Dean, D. C.; Nargund, R. P.; Patchett, A. A.; Smith, R. G. *Mol. Endocrinol.* **1996**, *10*, 57–61; (b) Sakamoto, T.; Moriya, M.; Tsuge, H.; Takahashi, T.; Haga, Y.; Nonoshita, K.; Okamoto, O.; Takahashi, H.; Sakuraba, A.; Hirohashi, T.; Shibata, T.; Kanno, T.; Ito, J.; Iwaasa, H.; Gomori, A.; Ishihara, A.; Fukuroda, T.; Kanatani, A.; Fukami, T. *Bioorg. Med. Chem.* **2009**, *17*, 5015–5026; (c) Horton, D. A.; Severinsen, R.; Kofod-Hansen, M.; Bourne, G. T.; Smythe, M. L. *J. Comb. Chem.* **2005**, *7*, 421–435; (d) Ong, H. H.; Profitt, J. A.; Fortunato, J.; Glamkowski, E. J.; Ellis, D. B.; Geyer, H. M., III; Wilker, J. C.; Burghard, H. *J. Med. Chem.* **1983**, *26*, 981–986; (e) Patchett, A. A.; Nargund, R. P.; Tata, J. R.; Chen, M.-H.; Barakat, K. J.; Johnston, D. B. R.; Cheng, K.; Chan, W. W.-S.; Butler, B.; Hickey, G.; Jacks, T.; Schleim, K.; Pong, S.-S.; Chaung, L.-Y. P.; Chen, H. Y.; Frazier, E.; Leung, K. H.; Chiu, S.-H. L.; Smith, R. G. *Proc. Natl. Acad. Sci. U.S.A.* **1995**, *92*, 7001–7005.
3. Piatnitski Chekler, E. L.; Khan, T. A.; Mamidala, R.; Anderson, J. T.; Tangirala, R. S.; Verhoest, P. R.; Gilbert, A. M. *Tetrahedron Lett.* **2012**, *53*, 377–379.
4. (a) Norberto, F.; Santos, S.; Silva, D.; Hervés, P.; Miguel, A. S.; Vilela, F. *J. Chem. Soc., Perkin Trans. 2* **2002**, 1162–1165; (b) Schneider, C.; Gueyrard, D.; Popowycz, F.; Joseph, B.; Goekjian, P. G. *Synlett* **2007**, 2237–2241; (c) Schmid, S.; Röttgen, M.; Thewalt, U.; Austel, V. *Org. Biomol. Chem.* **2005**, *3*, 3408–3421; (d) Bolhofer, W. A.; Deana, A. A.; Habecker, C. N.; Hoffman, J. M.; Gould, N. P.; Pietruszkiewicz, A. M.; Prugh, J. D.; Torchiana, M. L.; Cragoe, E. J., Jr.; Hirschmann, R. *J. Med. Chem.* **1983**, *26*, 544–548.
5. (a) Ito, F.; Hayashi, S.; Hashizume, Y.; Mihara S. PCT Int. Appl. WO/2005/016913, 2005. (b) Gao, Y.-D.; Macneil, D. J.; Yang, L.; Morin, N. R.; Fukami, T.; Kanatani, A.; Fukuroda, T.; Ishii, Y.; Morin, M. PCT Int. Appl. WO/2000/027845, 2000. (c) Cassayre, J.; Molleyres, L.-P.; Maienfisch, P.; Cederbaum, F. PCT Int. Appl. WO/2005/061512, 2005.
6. (a) Bodick, N. C.; Offen, W. W.; Levey, A. I.; Cutler, N. R.; Gauthier, S. G.; Satlin, A.; Shannon, H. E.; Tollefson, G. D.; Rasmussen, K.; Bymaster, F. P.; Hurley, D. J.; Potter, W. Z.; Paul, S. M. *Arch. Neurol.* **1997**, *54*, 465–473; (b) Shekhar, A.; Potter, W. Z.; Lightfoot, J.; Lienemann, J.; Dubé, S.; Mallinckrodt, C.; Bymaster, F. P.; McKinzie, D. L.; Felder, C. C. *Am. J. Psychiatry* **2008**, *165*, 1033–1039.
7. DFT calculation of acyl transfer from pyridyl nitrogen atom to other atoms, see: Larionov, E.; Mahesh, M.; Spivey, A. C.; Wei, Y.; Zipse, H. *J. Am. Chem. Soc.* **2012**, *134*, 9390–9399.
8. Frisch, M. J.; Trucks, G. W.; Schlegel, H. B.; Scuseria, G. E.; Robb, M. A.; Cheeseman, J. R.; Scalmani, G.; Barone, V.; Mennucci, B.; Petersson, G. A.; Nakatsuji, H.; Caricato, M.; Li, X.; Hratchian, H. P.; Izmaylov, A. F.; Bloino, J.; Zheng, G.; Sonnenberg, J. L.; Hada, M.; Ehara, M.; Toyota, K.; Fukuda, R.; Hasegawa, J.; Ishida, M.; Nakajima, T.; Honda, Y.; Kitao, O.; Nakai, H.; Vreven, T.; Montgomery, J. A., Jr.; Peralta, J. E.; Ogliaro, F.; Bearpark, M.; Heyd, J. J.; Brothers, E.; Kudin, K. N.; Staroverov, V. N.; Kobayashi, R.; Normand, J.; Raghavachari, K.; Rendell, A.; Burant, J. C.; Iyengar, S. S.; Tomasi, J.; Cossi, M.; Rega, N.; Millam, N. J.; Klene, M.; Knox, J. E.; Cross, J. B.; Bakken, V.; Adamo, C.; Jaramillo, J.; Gomperts, R.; Stratmann, R. E.; Yazyev, O.; Austin, A. J.; Cammi, R.; Pomelli, C.; Ochterski, J. W.; Martin, R. L.; Morokuma, K.; Zakrzewski, V. G.; Voth, G. A.; Salvador, P.; Dannenberg, J. J.; Dapprich, S.; Daniels, A. D.; Farkas, Ö.; Foresman, J. B.; Ortiz, J. V.; Cioslowski, J.; Fox, D. J. *Gaussian 09, Revision A.02*; Gaussian: Wallingford, CT.
9. Becke, A. B. *J. Chem. Phys.* **1993**, *98*, 5648–5652.
10. (a) Petersson, G. A.; Bennett, A.; Tensfeldt, T. G.; Al-Laham, T. G.; Shirley, W. A.; Mantzaris, J. *J. Chem. Phys.* **1988**, *89*, 2193–2218; (b) Petersson, G. A.; Al-Laham, M. A. *J. Chem. Phys.* **1991**, *94*, 6081–6090.
11. Zhao, Y.; Truhlar, D. *Theor. Chem. Acc.* **2008**, *120*, 215–241.
12. (a) Fukui, K. *Acc. Chem. Res.* **1981**, *14*, 363–368; (b) Hratchian, H. P.; Schlegel, H. B. *J. Chem. Theory Comput.* **2005**, *1*, 61–69.
13. (a) Miertus, S.; Scrocco, E.; Tomasi, J. *Chem. Phys.* **1981**, *55*, 117–129; (b) Tomasi, J.; Mennucci, B.; Cammi, R. *Chem. Rev.* **2005**, *105*, 2999–3093.